



CrossMark  
 click for updates

Cite this: *RSC Adv.*, 2015, 5, 103782

## Selective recovery of rare earth elements using chelating ligands grafted on mesoporous surfaces†

Justyna Florek,<sup>‡ab</sup> Ambreen Mushtaq,<sup>‡ac</sup> Dominic Larivière,<sup>\*ac</sup> Gabrielle Cantin,<sup>ac</sup> Frédéric-Georges Fontaine<sup>\*ac</sup> and Freddy Kleitz<sup>\*ab</sup>

Nowadays, rare earth elements (REEs) and their compounds are critical for the rapidly growing advanced technology sectors and clean energy demands. However, their separation and purification still remain challenging. Among different extracting agents used for REE separation, the diglycolamide (DGA)-based materials have attracted increasing attention as one of the most effective extracting agents. In this contribution, a series of new and element-selective sorbents were generated through derivatisation of the diglycolamide ligand (DGA), grafted to mesoporous silica and tested for the separation of rare earth elements. It is shown that, by tuning the ligand *bite angle* and its environment, it is possible to improve the selectivity towards specific rare earth elements.

Received 10th October 2015  
 Accepted 23rd November 2015

DOI: 10.1039/c5ra21027e

[www.rsc.org/advances](http://www.rsc.org/advances)

### Introduction

The rare earth elements (REEs) and their alloys are used in many modern technologies including notably the production of consumer electronics, computers, cell phones or network and communication devices.<sup>1</sup> Their unique electrochemical, luminescent and magnetic properties help to make these technologies perform with reduced weight and energy consumption, and give the devices greater efficiency, speed, performance, durability and thermal stability. As such, the global consumption rate and hence, the demand for pure REEs have dramatically increased over the past two decades. Since industrially useful ores contain several of the REEs among many other contaminants, including radioactive uranium and thorium, the separation and purification of these mixtures are needed for further industrial processes. However, the chemical properties of all REEs are quite similar which complicate their separation. Industrial purification involves either liquid–liquid (LLE), supported liquid (SLE) or solid phase (SPE) extraction procedures, which rely on association constants between ligands and REEs based essentially on the lanthanide contraction effect. In LLE, cation- (carboxylic acids, phosphoric acids) and anion-exchangers (amines, diketones) have been used to recover the

REEs.<sup>2</sup> However, this type of extraction utilizes large volume of solvents during the repeated cycles of extraction while generating a significant portion of undesired and radioactive waste. In comparison, SLE and SPE are greener approaches for REE extraction and purification as one of the liquid phase is reduced/eliminated. Recently, SLE resins containing impregnated ligands have been used for REE purification.<sup>3</sup> Among them, the diglycolamide (DGA) resin which consists of a DGA derivative (tetraoctyl DGA) impregnated on a solid support is nowadays one of the most commonly used systems for separation of REEs from other elements.<sup>4</sup> Regrettably, as the ligand is only supported on the stationary phase, leaching into the aqueous phase is frequently observed, limiting its reusability.

The challenge in separating REEs from environmental and industrial samples resides in the fact that REEs, but more specifically the lanthanides (Ln), have very similar physical and chemical properties. Indeed, while other oxidation states are synthetically available for the REEs, they tend to exist in environmental conditions as trivalent ions.<sup>5</sup> In addition, all of the REEs have similar radii size ranging from 74.5 (Sc<sup>3+</sup>) to 103.2 pm (La<sup>3+</sup>).<sup>6</sup> They have coordination numbers ranging from 6 to 9, and sometimes more. In order to satisfy their coordination sphere, they tend to coordinate different solvent molecules and have a predilection for chelating ligands.<sup>7</sup> This affects the solubility of REE complexes in various solvents and thus makes their purification by LLE less efficient. However, the Ln<sup>3+</sup> cations are highly Lewis acidic and easily coordinate nucleophiles to form stable complexes and they show a clear tendency towards oxygen donors, both in acidic and basic conditions, which can be advantageous for their efficient extraction.<sup>8</sup> It is documented that the best ligands used for extraction of REEs are mostly oxygen donors (*e.g.*, carboxylic acids, ketones, phosphoric acids).<sup>9</sup> In particular, the derivatives of DGA are

<sup>a</sup>Department of Chemistry, Université Laval, Quebec City, G1V 0A6, QC, Canada. E-mail: [freddy.kleitz@chm.ulaval.ca](mailto:freddy.kleitz@chm.ulaval.ca); [dominic.lariviere@chm.ulaval.ca](mailto:dominic.lariviere@chm.ulaval.ca); [frederic.fontaine@chm.ulaval.ca](mailto:frederic.fontaine@chm.ulaval.ca); Fax: +1-418-656-7916; Tel: +1-418-656-7812, 7250, 5140

<sup>b</sup>Centre de Recherche sur les Matériaux Avancés (CERMA), Université Laval, Quebec City, G1V 0A6, QC, Canada

<sup>c</sup>Centre en Catalyse et Chimie Verte (C3V), Université Laval, Quebec City, G1V 0A6, QC, Canada

† Electronic supplementary information (ESI) available: Experimental details and additional data. See DOI: 10.1039/c5ra21027e

‡ Contributed equally to this work.

used industrially for the selective extraction of REEs from aqueous solutions, as they are commonly recognised as effective and size selective binders of trivalent f-elements. They show high and rapid extraction even in strong acidic conditions ( $10^{-4}$  to  $10^0$  M in  $\text{HNO}_3$ ).<sup>10</sup> Notably, the DIAMEX industrial process uses DGA derivatives to selectively extract lanthanides during reprocessing of spent nuclear fuels.<sup>11</sup> The structural analysis of the complexes bearing the DGA ligands shows that REEs bind traditionally in a tridentate fashion, where each metal ion is coordinated by the three oxygen atoms of DGA-type ligands. The lanthanide ions (e.g., La, Yb, Ce) are sterically saturated in their nine-coordinate geometry with three DGA ligands.<sup>12</sup> The angle formed by chelate ligands, known as the *bite angle*, can greatly affect the binding properties of these ligands in the complexes (Fig. 1D).<sup>13</sup> Ligands with large *bite angles* will have a higher affinity for larger ions whereas smaller *bite angles* will favour coordination to smaller ions. However, it is expected that a chelating ligand bound to a solid surface by more than one anchor point will possess a rigid conformation and will exhibit less flexibility to adapt itself to the metal electronic requirements than in solution. Therefore, by the right tailoring of chemically similar chelating ligands and their grafting on solid supports, it should be possible for functional materials to exhibit selective affinities for smaller or larger ions.

## Experimental

### Ligands synthesis

**Synthesis of 3,6-dioxaoctanedioic acid (DOODA acid).**<sup>14</sup> 20 ml of  $\text{HNO}_3$  was heated to 40–45 °C, under ambient atmosphere, and 7.0 g (0.046 mol) of triethylene glycol was added over 1 h. The temperature of the reaction was raised to 60–70 °C releasing orange fumes in the process. After the addition was complete, the reaction was cooled down to 40–45 °C then heated at 80 °C for 1 h. The acid formed was evacuated under vacuum for 1 h at 80 °C to get rid of all the nitrogen oxides. The light yellow oil solidified into a white sticky solid overnight (6.95 g, yield = 85%).  $^1\text{H}$  NMR (acetone- $d_6$ ).  $\delta$  (ppm) 4.15 (s, 4H,  $\text{CH}_2\text{-C=O}$ ), 3.73 (s, 4H,  $\text{CH}_2\text{-O}$ ).  $^{13}\text{C}$  NMR (acetone- $d_6$ ).  $\delta$  170.9 (s,  $\text{C=O}$ ), 70.4 (s,  $\text{CH}_2\text{-C=O}$ ), 67.6 (s,  $\text{CH}_2\text{-O}$ ).

**Synthesis of 3,6-dioxaoctanedioylchloride (DOODACl).** To 6.0 g (33 mmol) of 3,6-dioxaoctanedioic acid was added 60  $\mu\text{l}$  of DMF. 16 ml (26.2 g, 0.22 mol) of  $\text{SOCl}_2$  was added slowly to the

acid mixture while stirring. The reaction was refluxed for 4 h at 80 °C. The reaction was cooled down and put under vacuum for 1 h to remove the excess of  $\text{SOCl}_2$ . The yellow oil left behind was dissolved in  $2 \times 10$  ml of benzene and the solution was filtered. The filtrate was evaporated to give a light yellow oil that was crystallized from a mixture of pentane and ether at  $-30$  °C (6.30 g, yield = 87%).  $^1\text{H}$  NMR (benzene- $d_6$ ).  $\delta$  3.76 (s, 4H,  $\text{CH}_2\text{-C=O}$ ), 3.09 (s, 4H,  $\text{CH}_2\text{-O}$ ).  $^{13}\text{C}$  NMR (benzene- $d_6$ ).  $\delta$  171.7 (s,  $\text{C=O}$ ), 76.1 (s,  $\text{CH}_2\text{-C=O}$ ), 70.9 (s,  $\text{CH}_2\text{-O}$ ).

**Synthesis of 3,6-dioxaoctanediamido-propyltriethoxysilane (DOODA-APTS).** 2.00 g (9.30 mmol) of DOODACl was dissolved in 25 ml of toluene and cooled down to 0 °C. The solution was slowly added to a mixture of 4.57 ml (4.32 g, 0.195 mol) of APTS and 12.6 ml (9.10 g, 0.893 mol) of triethylamine in 20 ml of toluene. The reaction was allowed to warm to room temperature overnight. The reaction was filtered and the filtrate was evaporated and dried under vacuum to give 3.00 g of thick yellow oil (yield = 96%).  $^1\text{H}$  NMR (benzene- $d_6$ ).  $\delta$  6.61 (br, 2H,  $\text{NH}^{\text{APTS}}$ ), 3.77 (m, 16H,  $\text{CH}_2\text{-O-Si}^{\text{APTS}}$ ,  $\text{CH}_2\text{-C=O}$ ), 3.32 (q, 4H,  $\text{CH}_2\text{-NH}^{\text{APTS}}$ ), 3.00 (s, 4H,  $\text{CH}_2\text{-O}$ ), 1.72 (m, 4H,  $\text{CH}_2\text{-CH}_2^{\text{APTS}}$ ), 1.16 (t, 18H,  $\text{CH}_3^{\text{APTS}}$ ), 0.65 (t, 4H,  $\text{CH}_2\text{-Si}^{\text{APTS}}$ ).  $^{13}\text{C}$  NMR (benzene- $d_6$ ).  $\delta$  168.6 (s,  $\text{C=O}$ ), 71.1 (s,  $\text{CH}_2\text{-C=O}$ ), 70.4 (s,  $\text{CH}_2\text{-O}$ ), 58.5 (s,  $\text{CH}_2\text{-O-Si}^{\text{APTS}}$ ), 41.5 (s,  $\text{CH}_2\text{-NH}^{\text{APTS}}$ ), 23.8 (s,  $\text{CH}_2\text{-CH}_2^{\text{APTS}}$ ), 18.5 (s,  $\text{CH}_3^{\text{APTS}}$ ), 8.2 (s,  $\text{CH}_2\text{-Si}^{\text{APTS}}$ ).

**Synthesis of 2,5-furandioylchloride (FDGACl).**<sup>15</sup> To 2.50 g (16.0 mmol) of 2,5-furandicarboxylic acid was added 50  $\mu\text{l}$  of DMF. 5 ml (8.19 g, 68.8 mmol) of  $\text{SOCl}_2$  was added slowly to the acid mixture while stirring. The reaction was refluxed for 6 h at 80 °C. The reaction was cooled down and put under vacuum for 1 h to remove excess of  $\text{SOCl}_2$ . A white crystalline solid was obtained. The solid was sublimated at 75 °C to give 2.74 g of product (yield = 89%).  $^1\text{H}$  NMR (benzene- $d_6$ ).  $\delta$  6.22 (s, 2H, CH).  $^{13}\text{C}$  NMR (benzene- $d_6$ ).  $\delta$  155.4 (s,  $\text{C=O}$ ), 148.7 (s, C-O), 122.7 (s, CH).

**Synthesis of furan-2,4-diamido-propyltriethoxysilane (FDGA-APTS).** 2.00 g (10.4 mmol) of FDGACl was dissolved in 25 ml of toluene and to the solution was slowly added a mixture of 5.07 ml (4.79 g, 21.8 mmol) of APTS and 14.4 ml (10.4 g, 103 mmol) of triethylamine in 20 ml of toluene. The reaction was put under reflux at 90 °C overnight. The reaction was cooled, filtered and the filtrate was evaporated and dried under vacuum to give 5.65 g of a white solid (yield = 96%).  $^1\text{H}$  NMR (benzene- $d_6$ ).  $\delta$  7.26 (br, 2H,  $\text{NH}^{\text{APTS}}$ ), 6.95 (s, 2H, CH), 3.74 (q, 12H,  $\text{CH}_2\text{-O-Si}^{\text{APTS}}$ ), 3.40 (q, 4H,  $\text{CH}_2\text{-NH}^{\text{APTS}}$ ), 1.76 (m, 4H,  $\text{CH}_2\text{-CH}_2^{\text{APTS}}$ ), 1.14 (t, 18H,  $\text{CH}_3^{\text{APTS}}$ ), 0.65 (t, 4H,  $\text{CH}_2\text{-Si}^{\text{APTS}}$ ).  $^{13}\text{C}$  NMR (benzene- $d_6$ ).  $\delta$  158.1 (s,  $\text{C=O}$ ), 149.4 (s, C-O), 114.9 (s, CH), 58.5 (s,  $\text{CH}_2\text{-O-Si}^{\text{APTS}}$ ), 42.0 (s,  $\text{CH}_2\text{-NH}^{\text{APTS}}$ ), 23.8 (s,  $\text{CH}_2\text{-CH}_2^{\text{APTS}}$ ), 18.5 (s,  $\text{CH}_3^{\text{APTS}}$ ), 8.3 (s,  $\text{CH}_2\text{-Si}^{\text{APTS}}$ ).

**Synthesis of diglycolyl chloride (DGACl).** To 5.00 g (0.037 mol) of diglycolic acid was added 15 ml of  $\text{CH}_2\text{Cl}_2$  and 40  $\mu\text{l}$  of DMF. 17.4 ml (25.8 g, 0.200 mol) of  $\text{C}_2\text{O}_2\text{Cl}_2$  was added slowly to the acid mixture while stirring in an ice bath. The reaction was allowed to warm up overnight. The reaction mixture was then distilled under nitrogen at 100 °C to distil off the excess of  $\text{C}_2\text{O}_2\text{Cl}_2$  and  $\text{CH}_2\text{Cl}_2$ . A yellow oil was recovered (5.50 g, yield = 88%).  $^1\text{H}$  NMR (benzene- $d_6$ ).  $\delta$  3.47 (s, 4H,  $\text{CH}_2\text{-O}$ ).  $^{13}\text{C}$  NMR (benzene- $d_6$ ).  $\delta$  170.5 (s,  $\text{C=O}$ ), 74.7 (s,  $\text{CH}_2\text{-O}$ ).

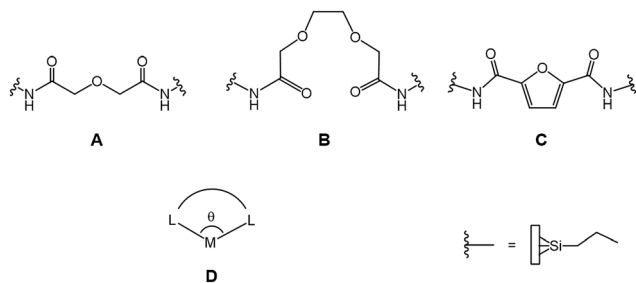


Fig. 1 (A) DGA, (B) DOODA and (C) FDGA ligands grafted on silica (KIT-6). (D) *Bite angle* between the metal and the coordinating atoms of the ligand.

**Synthesis of diglycol-2,4-diamido-propyltriethoxysilane (DGA-APTS).** 600 mg (3.51 mmol) of DGACl was dissolved in 15 ml of toluene and was cooled down to 0 °C. To the solution was slowly added a mixture of 1.72 ml (1.63 g, 7.36 mmol) of APTS and 4.89 ml (3.55 g, 35.1 mmol) of triethylamine in 10 ml of toluene. The reaction was allowed to warm to room temperature overnight. The reaction was filtered and the filtrate was evaporated and dried under vacuum to give 1.37 g of a thick yellow oil (yield = 89%). <sup>1</sup>H NMR (benzene-d<sub>6</sub>). δ 7.52 (br, 2H, NH<sup>APTS</sup>), 3.89 (4H, CH<sub>2</sub>-O), 3.75 (q, 12H, CH<sub>2</sub>-OSi<sup>APTS</sup>), 3.31 (q, 4H, CH<sub>2</sub>-NH<sup>APTS</sup>), 1.75 (m, 4H, CH<sub>2</sub>-CH<sub>2</sub><sup>APTS</sup>), 1.15 (t, 18H, CH<sub>3</sub><sup>APTS</sup>), 0.67 (t, 4H, CH<sub>2</sub>-Si<sup>APTS</sup>). <sup>13</sup>C NMR (benzene-d<sub>6</sub>). δ 169.0 (s, C=O), 71.6 (s, CH<sub>2</sub>-O), 58.5 (s, CH<sub>2</sub>-OSi<sup>APTS</sup>), 41.8 (s, CH<sub>2</sub>-NH<sup>APTS</sup>), 23.6 (s, CH<sub>2</sub>-CH<sub>2</sub><sup>APTS</sup>), 18.5 (s, CH<sub>3</sub><sup>APTS</sup>), 8.3 (s, CH<sub>2</sub>-Si<sup>APTS</sup>).

**Synthesis of *N,N*-dioctyl-3,6-dioxaoctanediamide (TODOODA).**<sup>11b</sup> 315 mg (1.46 mmol) of DOODACl in 5 ml of benzene was added dropwise to a solution *N,N*-dioctylamine (840 mg, 1.05 ml, 3.48 mmol) and triethylamine (2.21 g, 3.04 ml, 21.8 mmol) in 30 ml of benzene at 0 °C. The reaction was allowed to warm to room temperature overnight. The reaction was evaporated and then extracted with 3 × 10 ml of hexane. Evaporation of the hexane filtrate gave 802 mg of a yellow oil (yield = 87%). <sup>1</sup>H NMR (chloroform-d). δ 4.20 (s, 4H, CH<sub>2</sub>-C=O), 3.76 (s, 4H, CH<sub>2</sub>-O), 3.23 (dt, 8H, CH<sub>2</sub>-N<sup>octyl</sup>), 1.52 (br, 8H, CH<sub>2</sub>-CH<sub>3</sub><sup>octyl</sup>), 1.27 (s, 40H, CH<sub>2</sub><sup>octyl</sup>), 0.87 (t, 12H, CH<sub>3</sub><sup>octyl</sup>). <sup>13</sup>C NMR (chloroform-d). δ 168.5 (s, C=O), 77.1 (s, CH<sub>2</sub>-C=O), 69.7 (s, CH<sub>2</sub>-O), 45.7 (d, CH<sub>2</sub>N), 31.7, 29.2, 28.8, 27.5, 26.9 (CH<sub>2</sub>), 22.5 (s, CH<sub>2</sub>-CH<sub>3</sub>), 14.0 (s, CH<sub>3</sub>).

**Synthesis of *N,N*-dioctylfuran-2,4-diamide (TOFDGA).** 300 mg (1.55 mmol) of FDGACl in 10 ml of THF was added dropwise to a solution *N,N*-dioctylamine (1.17 ml, 0.937 g, 3.88 mmol) and triethylamine (2.15 ml, 1.56 g, 15.4 mmol) in 30 ml of THF at 0 °C. The reaction was allowed to warm to room temperature overnight. The reaction was evaporated and the residue was dissolved in 30 ml of dichloromethane and extracted with 3 × 20 ml of 5% HCl in water. The organic fraction was dried on MgSO<sub>4</sub>, filtered and evaporated to give 845 mg of a yellow oil (yield = 90%). <sup>1</sup>H NMR (chloroform-d). δ 6.93 (s, 2H, CH), 3.46 (br, 8H, CH<sub>2</sub>-N<sup>octyl</sup>), 1.60 (br, 8H, CH<sub>2</sub>-CH<sub>3</sub><sup>octyl</sup>), 1.26 (s, 40H, CH<sub>2</sub><sup>octyl</sup>), 0.88 (t, 12H, CH<sub>3</sub><sup>octyl</sup>). <sup>13</sup>C NMR (chloroform-d). δ 159.6 (s, C=O), 148.6 (s, CH), 115.6 (s, CO), 46.7 (d, CH<sub>2</sub>N), 31.7, 29.2, 27.5, 27.0, 26.7 (CH<sub>2</sub>), 22.6 (s, CH<sub>2</sub>-CH<sub>3</sub>), 14.0 (s, CH<sub>3</sub>).

### Materials synthesis and functionalization

Following our previous success with actinide/lanthanide adsorption, we selected high-surface area KIT-6 silica (with a 3-D open pore structure) as a suitable support for the chelating ligands.<sup>16</sup> High quality KIT-6 silica materials were obtained following the procedure reported by Kleitz *et al.*<sup>17</sup> Briefly, 9.0 g of Pluronic P123 (EO<sub>20</sub>PO<sub>70</sub>EO<sub>20</sub>, Sigma-Aldrich) was dissolved in 325.0 g of distilled water and 17.4 g HCl (37%) was added under vigorous stirring. After complete dissolution, 9.0 g of *n*-butanol (BuOH, Aldrich, 99%) was added. The reaction mixture was left under stirring at 35 °C for 1 h, after which 19.4 g of tetraethoxysilane (TEOS, Sigma-Aldrich, 99%) was added at once to

the homogenous clear solution. The molar composition of the starting mixture was TEOS/P123/HCl/H<sub>2</sub>O/BuOH = 1.0/0.017/1.83/195/1.31. This mixture was left under stirring at 35 °C for 24 h, followed by an aging step at 100 °C for 24 h under static conditions. After, the resulting solid product was filtered and dried for 24 h at 100 °C. From the as-synthesized KIT-6 material, the template was removed by extraction in ethanol-HCl mixture, followed by calcination in air at 550 °C. Prior to the grafting procedure, the KIT-6 support (1.0 g) was activated overnight at 150 °C under vacuum and then dispersed in 100 ml of dry toluene, under N<sub>2</sub> flow. After 2 h, the solution of the chosen silane-modified ligand (600 mg of DGA-APTS or 600 mg of DOODA-APTS or 300 mg of FDGA-APTS) and 1.2 ml of triethylamine (Alfa Aesar, 99%) was added at once to this suspension, under inert atmosphere. The resulting mixture was left under reflux conditions for 24 h. In case of the DOODA ligand, the grafting procedure was performed at room temperature for an extended period of the time (48 h). After the modification procedure, the functionalized silica product was filtered, washed thoroughly with toluene and then dried at 60 °C overnight in air. Unreacted silane molecules were removed by Soxhlet extraction in dichloromethane for 6 h. The resulting products are noted as KIT-6-N-DGA, KIT-6-N-FDGA or KIT-6-N-DOODA, respectively.

### Characterization techniques

N<sub>2</sub> adsorption-desorption isotherms were measured at -196 °C (77 K) using an Autosorb-iQ2 sorption analyzer (Quantachrome Instruments, Boynton Beach, USA). Prior to the analysis, the samples were outgassed for 10 h at 200 °C (unmodified silica support) or at 80 °C for 12 h (functionalized sorbents). The specific surface area (*S*<sub>BET</sub>) was determined using the Brunauer-Emmett-Teller equation in the range 0.05 ≤ *P*/*P*<sub>0</sub> ≤ 0.20 and the total pore volume (*V*<sub>pore</sub>) was measured at *P*/*P*<sub>0</sub> = 0.95. The pore size distributions for all materials were calculated by using the nonlocal density functional theory (NLDFT) method (Autosorb ASiQWin software) considering the sorption of nitrogen at -196 °C in silica with cylindrical pores.<sup>18</sup> The pore widths were determined by applying the NLDFT kernel of equilibrium isotherms (desorption branch). <sup>13</sup>C cross-polarization (CP/MAS) and <sup>29</sup>Si magic-angle-spinning (MAS) nuclear magnetic resonance (NMR) analyses were carried out on a Bruker Avance 300 MHz spectrometer (Bruker Biospin Ltd, Milton, Canada) at 75.4 MHz for <sup>13</sup>C and 59.6 MHz for <sup>29</sup>Si. <sup>29</sup>Si MAS NMR spectra were recorded with a spin echo sequence to avoid instrument background with a recycle delay of 30 seconds in a 4 mm rotor spin at 8 kHz. <sup>13</sup>C CP/MAS NMR spectra were recorded with a 4 mm MAS probe with a spinning rate of 8 kHz and contact time of 1 ms. Chemical shifts were referenced to tetramethylsilane (TMS) for <sup>29</sup>Si and adamantane for <sup>13</sup>C. Simultaneous thermogravimetric analysis-differential scanning calorimetry analysis (TGA-DTA/DSC) was performed using a Netzsch STA 449C thermogravimetric analyzer, under air flow of 20 ml min<sup>-1</sup> and with temperature-programmed heating rate of 10 °C min<sup>-1</sup>. Elemental analysis was performed by the combustion method using a CHNS Analyzer Flash 2000, Thermo Scientific. X-ray

photoelectron spectroscopy (XPS) measurements were conducted on a Kratos AXIS-ULTRA spectrometer with a monochromatic Al X-ray source operated at 300 W. High energy resolution spectra (N 1s) were recorded at 20 eV or 40 eV pass energy and step size of 0.05 eV or 0.1 eV.

**Extraction methodology.** Extraction behaviour of REEs and other metals were investigated on DGA resin-normal (*N,N,N',N'*-tetra-*n*-octyldiglycolamide resin; Eichrom; USA Lisle, IL), on unfunctionalized and DGA, DOODA and FDGA moieties tethered on a mesoporous support (KIT-6, KIT-6-N-DGA, KIT-6-N-DOODA and KIT-6-N-FDGA, respectively). Extraction experiments were performed either as a batch or flow-through mode. LLE experiments were also performed in order to determine the effect of tethering the ligand on the extractive properties. Elemental quantification of the various elements was performed by ICP-MS (Model 8800, Agilent Technologies). The initial and final concentrations of the REEs and additional elements in solutions were determined and used to calculate either extraction capacity or distribution constant ( $K_d$ ).

**Batch extraction studies, SLE and SPE system.** A 15  $\mu\text{g l}^{-1}$  solution of REEs containing additional metals (Al, Fe, U, Th) in  $\text{HNO}_3$  (pH = 4) was prepared from the reference standard solutions (Plasma, Cal, SCP Science). The solution/solid ratio was fixed to 500 ( $\text{V m}^{-1}$ ). The samples (10 mg) were stirred in an orbital shaker for 30 min and the supernatant was subsequently filtered through a 0.2  $\mu\text{m}$  syringe filter. All experiments were done in triplicates and only the average values are provided.

**Batch extraction studies, LLE system.** A commercial Micro-Kros hollow fiber module was used (Spectrum Labs, USA) for the non-dispersive solvent extraction (NDSX) experiment. The total surface area was 11  $\text{cm}^2$  with 6 polysulfone fibers. Both phases, aqueous and organic, were contacted in counter-current in the hollow fiber module and extraction occurs in the pores of the fibers' wall. The aqueous solution was agitated continuously to ensure uniform concentration while the organic solution was circulated as a closed loop. 12  $\mu\text{mol}$  of TODGA, TODOODA or FDGA was added to 2.4 ml of dodecane, whereas 3 M nitric acid containing 100  $\mu\text{g l}^{-1}$  of each REE was prepared from a standard solution (100  $\text{mg l}^{-1}$ ; Plasma, Cal, SCP Science) by appropriate dilution, and used as aqueous phase. After the optimization of the ICP measurements, the 100  $\mu\text{g l}^{-1}$  solution of REEs was used in our experimental setup. Both phases (2.4 ml each) were recirculated for 90 minutes by a peristaltic pump through the lumen side (aqueous phase) and the shell side (organic phase) of the fiber module. The organic phase flow rate was kept between 600 and 1200  $\mu\text{l min}^{-1}$  whereas the aqueous phase flow was set between 135  $\mu\text{l min}^{-1}$  and 185  $\mu\text{l min}^{-1}$ .

**Europium extraction studied in flow system.** Extraction capacity studies of various SLE and SPE alternatives were performed using a solution of 100  $\mu\text{g l}^{-1}$  of europium standard (Plasma, Cal, SCP Science). For the extraction tests, 150 mg of DGA-resin-normal and 30 mg of mesoporous sorbents were packed inside 2 ml SPE cartridges through a slurry-packing method. Filled cartridges were washed with high purity water (10 ml) and conditioned with  $\text{HNO}_3$  pH = 4 (mesoporous sorbents) or 3 M  $\text{HNO}_3$  (commercial resin), then the solution of

europium was loaded and passed through the column, with the flow rate 1  $\text{ml min}^{-1}$ .

**Sorbent reusability studies.** For the reusability studies, 200 ml of a solution of 1  $\text{mg l}^{-1}$  of europium was passed through the analytical setup presented in the previous section and the unretained Eu analyzed by ICP-MS. Subsequently, the sorbent was washed with 0.1 M  $(\text{NH}_4)_2\text{C}_2\text{O}_4$  (10 ml) and high purity water (20 ml). The material was then reconditioned with  $\text{HNO}_3$  and used in the subsequent extraction tests by repeating the above mentioned procedure, to achieve 10 extraction-elution cycles.

## Results and discussion

Recently, we have studied the effect of the chemical anchoring of chelating ligands on mesoporous silica supports for the selective extraction of actinides and trivalent f-element ions.<sup>16</sup> It was found that anchored phosphonate ligands were highly efficient in extracting uranium from acidic media. Anchoring a DGA ligand (diglycol-2,4-diamido-propyltriethoxysilane, Fig. 1A) on KIT-6 also demonstrated improved extractive properties for all REEs in comparison to SLE resin while exhibiting enhanced selectivity for some of them. In addition, the tethering of DGA on the silica surface overcomes the leaching of the ligand observed in SLE providing a greater reusability of the resin. Our previous results also suggest that the mid-size ions (*e.g.*, Eu and Gd) have greater affinity for the tethered DGA than smaller and larger ions. Therefore, there is a need for the preparation of materials where the grafted ligands would have tailored *bite angles* for the selective extraction of larger or smaller REEs. To achieve this goal, new hybrid mesoporous materials containing DOODA (3,6-dioxaoctanediamidopropyltriethoxysilane) and FDGA (furan-2,4-diamidopropyltriethoxysilane) (Fig. 1B and C) ligands were developed in order to explore the influence of their *bite angle* and rigidity on the selective extraction of REEs.

The DOODA and FDGA ligands were synthesized using a slightly modified reported protocol<sup>14a,15,19</sup> and by modification of the corresponding acid chlorides with 3-aminopropyltriethoxysilane (APTS) (see ESI†). The modification of the ligand with APTS on both sides was confirmed by the appearance of a broad peak at  $\delta$  (ppm) = 6.61 for DOODA and 7.26 for FDGA in the  $^1\text{H}$  NMR spectrum, each integrating for two protons corresponding to the NH group. In  $^{13}\text{C}$  NMR, the disappearance of the carbonyl peaks at  $\delta$  = 171.7 (DOODACL), 155.4 (FDGACL) and their appearance at  $\delta$  = 168.6 (DOODA-APTS), 158.1 (FDGA-APTS) also confirmed the formation of amide bond. These ligands were then grafted on large pore mesoporous KIT-6 silica support.<sup>17,18a</sup>

After grafting, the resulting hybrid materials demonstrate typical type IV isotherms with a steep capillary condensation step and a hysteresis loop (type H1 adsorption-desorption hysteresis) in the relative pressure range  $P/P_0$  of 0.6–0.8, which is characteristic of mesoporous solids with large cylindrical mesopores (>4 nm)<sup>20</sup> (Fig. 2). After anchoring of the organic ligands on the silica surface, the shape of the hysteresis loop was well maintained and shifted to the lower values of relative

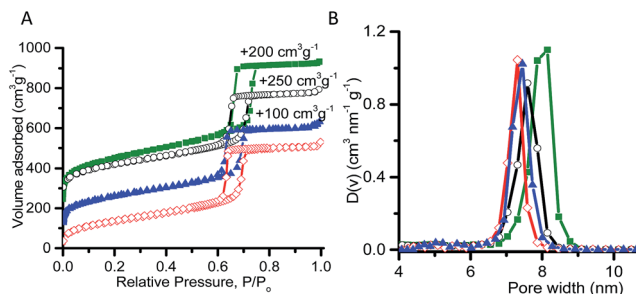


Fig. 2 N<sub>2</sub> adsorption-desorption isotherms at -196 °C for synthesized materials (A) and respective pore size distributions calculated from the desorption branch using the NLDFT method (silica with cylindrical pore model) (B). KIT-6 (green); KIT-6-N-DGA (black); KIT-6-N-DOODA (blue); KIT-6-N-FDGA (red).

pressure ( $P/P_0$ ), indicative of a decrease in the pore size upon surface modification. The physicochemical characteristics of the hybrid sorbents are compiled in Table 1. The KIT-6-N-DGA sample exhibits the highest BET specific surface area, 621 m<sup>2</sup> g<sup>-1</sup>, compared to the two other mesoporous sorbents, *i.e.*, 588 m<sup>2</sup> g<sup>-1</sup> for KIT-6-N-DOODA and 502 m<sup>2</sup> g<sup>-1</sup> for KIT-6-N-FDGA respectively. For all the materials, upon surface modification, the pore widths of the synthesized sorbents become smaller and similar gradual decrease is observed for the pore volume, compared to the parent silica.

The structure of the anchored ligands was established by solid-state NMR spectroscopy (Fig. 3A and B, Table S1, ESI<sup>†</sup>). The peaks corresponding to the ligands were clearly observed in the <sup>13</sup>C CP/NMR spectra and were in accordance with those observed in liquid <sup>13</sup>C NMR of the APTS-modified ligands. The covalent attachment of the ligands to the surface was confirmed by <sup>29</sup>Si MAS NMR revealing signals at about -50, -58, and -67 ppm corresponding to T<sup>1-3</sup> species as (SiO)(OR)<sub>2</sub>Si-R, (SiO)<sub>2</sub>(OR)Si-R, (SiO)<sub>3</sub>Si-R; indicating that the ligands are covalently anchored to the surface through the silanol groups.<sup>21</sup> The <sup>29</sup>Si MAS NMR spectrum of KIT-6-N-FGDA showed only the presence of T<sup>1</sup> species, whereas the spectra of KIT-6-N-DOODA and KIT-6-N-DGA materials show the presence of a mixture of mono- and bipodal, and bi- and tripodal attachment for each extremity of the ligand, respectively for these two materials. Further, the composition of the organic moieties attached to the silica surface was verified by thermogravimetry and by CHN elemental analysis. The highest organic content, determined by

Table 1 Physicochemical parameters derived from N<sub>2</sub> physisorption measurements at low temperature (-196 °C)

Material	$S_{\text{BET}}$ (m <sup>2</sup> g <sup>-1</sup> )	Pore size <sup>a</sup> (nm)	$V_{\text{pore}}^b$ (cm <sup>3</sup> g <sup>-1</sup> )
KIT-6	910	8.1	1.21
KIT-6-N-DGA	621	7.6	0.82
KIT-6-N-DOODA	588	7.4	0.78
KIT-6-N-FDGA	502	7.3	0.78

<sup>a</sup> Values obtained from the NLDFT method, based on the desorption branch. <sup>b</sup> Total pore volume determined at  $P/P_0 = 0.95$ .

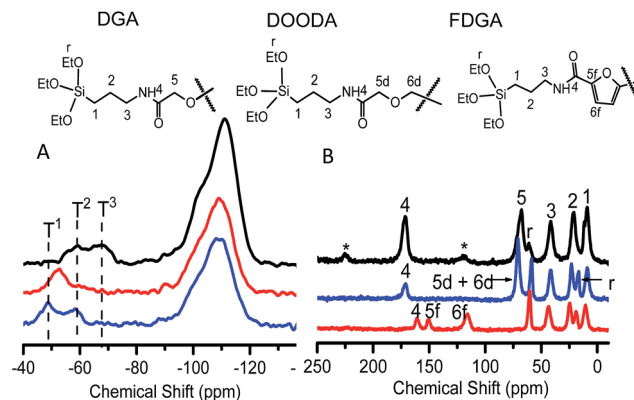


Fig. 3 <sup>29</sup>Si MAS NMR and <sup>13</sup>C CP/NMR spectra of the ligand-modified KIT-6 materials (KIT-6-N-DGA black, KIT-6-N-DOODA blue, KIT-6-N-FDGA red). The two additional bands (\*) visible on the <sup>13</sup>C NMR spectra of KIT-6-DGA material are spinning side-bands of the carbonyl carbon.

a total mass loss of 24%, was found for the KIT-6-N-DGA hybrid material (Table 2). The KIT-6-N-DOODA and KIT-6-N-FDGA sorbents showed weight loss profiles being about 22% and 16%, respectively. The amounts of carbon, nitrogen and hydrogen for all the modified samples were obtained by CHN elemental analysis and the respective values are given in Table 2. Based on the data obtained from the low temperature N<sub>2</sub> sorption and elemental analysis, it was possible to calculate the apparent surface density of the ligands (Table 2). The highest apparent surface density was estimated for KIT-6-N-DGA, while the lowest surface density of ligand was found for the KIT-6-N-FDGA sorbent, in agreement with the TGA mass loss observed for these materials. Note that, these surface density values do not take into account the accessibility of the ligand, but only provide a relative coverage of the silica surface by the different ligands.

First, the performance of the synthesized mesoporous sorbents, in comparison to the commercial DGA resin, was studied in the dynamic (flow) system for one selected element – europium. Our results, similar to data published by others,<sup>22</sup> showed that the DGA-normal resin has a capacity of 0.21 mmol Eu g<sup>-1</sup> towards europium. Superior extraction abilities were

Table 2 Total amount of ligand introduced by grafting for the different functionalized samples, based on TGA and CHN analysis and estimated surface density of the ligands

Sample	Mass loss <sup>a</sup> (%)	CHN (%)			Density of the ligand <sup>b</sup> (nm <sup>-2</sup> )
		C	N	H	
KIT-6-N-DGA	24	13.60	2.58	2.53	0.83
KIT-6-N-DOODA	22	14.74	1.92	2.35	0.73
KIT-6-N-FDGA	16	6.53	0.89	1.19	0.46

<sup>a</sup> Determined by TGA-DSC analysis in temperature range 140–650 °C. <sup>b</sup> Calculated using N content (CHN analysis) and specific surface area ( $S_{\text{BET}}$ ).

**Table 3** Extraction capacity of different mesoporous sorbents and commercial DGA resin in the dynamic system

Material	Eu extraction (mmol g <sup>-1</sup> )
DGA-normal resin	0.21
KIT-6-N-DGA	1.10
KIT-6-N-DOODA	0.99
KIT-6-N-FDGA	0.49

calculated for all the synthesized mesoporous sorbents (Table 3). In comparison, extraction capacity five times higher was obtained for KIT-6-N-DGA (1.10 mmol Eu g<sup>-1</sup>), which possesses the highest amount of the ligand (24% mass loss from TGA analysis). A slightly lower Eu uptake of 0.99 mmol Eu g<sup>-1</sup> was observed for KIT-6-N-DOODA (22% mass loss from TGA), and the lowest europium uptake was found for KIT-6-N-FDGA material (0.49 mmol Eu g<sup>-1</sup>). Nevertheless, the latter value still is significantly above the extraction capacity of the commercial resin.

The functionalized materials were further tested for extraction of REEs from a mixture of lanthanides, uranium, thorium and additional metal ions (*i.e.*, Al<sup>3+</sup>, Fe<sup>3+</sup>). The values of the partition coefficients ( $K_d$ ) for REEs and other relevant elements obtained through batch extraction are plotted in Fig. 4 (see also Fig. S19, ESI†). The tabulated data can be found in Table S2, ESI†. The  $K_d$  values for KIT-6-N-DGA are also presented for comparison purposes. From the results obtained, it is clear that all functionalized KIT-6 materials show higher  $K_d$  values for lanthanides in comparison to other competing ions commonly present in environmental and mining wastes. We also observe that the hybrid materials have generally lower  $K_d$  for U and Th ions (with the exception of KIT-6-N-FGDA), thus limiting the

preconcentration of these radioactive elements with the REEs. This should translate into an easier management of contaminated wastes during the REEs separation process. This selectivity to REEs reflects the effect of introducing rigidity in the ligand (through immobilisation onto a solid support) on its chelating properties. While KIT-6-N-DGA exhibits selectivity for Eu<sup>3+</sup>, Gd<sup>3+</sup> and Tb<sup>3+</sup>, which are mid-size lanthanides with atomic radii of 94.7, 93.8, and 92.3 pm, respectively, KIT-6-N-DOODA shows selectivity towards smaller lanthanides. Indeed, for the latter material, the  $K_d$  values are high for REEs from holmium to lutetium with values exceeding 5100 ml g<sup>-1</sup>. Although the same geometric parameters cannot be used to compare a tridentate and a tetradentate ligand, it was observed that for La-DOODA complexes the angle between adjacent coordination sites ranges between 57.90–58.27°, while for the DGA-La complexes larger angles are observed at 60.35–60.93°. <sup>11b,12b</sup> The DOODA ligand has four coordinating oxygen atoms and coordinates metal ions in a tetradentate geometry. It is believed that, this small tetradentate pocket provides an appropriate *bite angle* favouring coordination to the smaller lanthanides.

Considering the extraction properties of DOODA in liquid-liquid extraction, it was observed that, under the conditions tested, the  $K_d$  decreases from La to Lu (Fig. 4B), therefore showing greater selectivity of DOODA for larger ions. This selectivity was found to be sensitive to the concentration of HNO<sub>3</sub>, water and the nature and concentration of the ligand. <sup>23</sup> For example, tetraoctyl(TO)DGA in LLE is has higher  $K_d$  (Fig. 4A), thus showing higher selectivity for smaller lanthanides. <sup>10b,24</sup> In contrast, in our solid-state system, DGA becomes more efficient for extracting middle lanthanides. These differences in our system and LLE can be attributed to the change in the coordination sphere of the lanthanide ions, and the nature of ligand binding them. In solution, the number of ligands coordinated to lanthanide ions is sensitive to the concentration of ligand, HNO<sub>3</sub> and water. Three to four ligand molecules form complexes with lanthanide ions along with water and nitrate ions (NO<sub>3</sub><sup>-</sup>) in the coordination sphere. Since the lighter lanthanides have higher hydration energy, they tend to have more water molecules in their coordination sphere and are thus extracted less in non-polar solvents. The smaller/heavier lanthanides have less hydration energy and small coordination sphere and are therefore extracted more. <sup>25</sup> While as in our system, the number of ligands coordinating to the metal cannot change as they are immobilised on the pore surface, and hence, only those metal ions which may bind stronger with the ligand (*i.e.*, have an appropriate radius for the *bite angle* of the ligand) will be efficiently trapped; the others will easily be eluted. This strikingly distinct behaviour of the DOODA and DGA ligands in our SPE system is thus attributed to the chemical anchoring of the ligand to the solid surface that decreases the flexibility of the coordinating carbonyl groups and further adds to the overall rigidity of the ligand. This effect seems to provide a more fixed *bite angle* to the ligand yielding a more pronounced discriminating effect towards REE cations. Moreover, it is also seen that the  $K_d$  value of TOFDGA in LLE is higher for larger lanthanide ions and subsequently decreases along the series. Thus, as

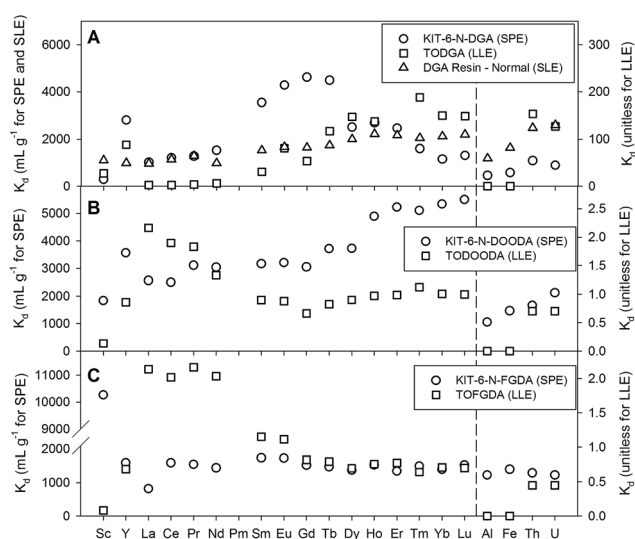


**Fig. 4** Distribution coefficient ( $K_d$ ) values for functionalized hybrid materials (SPE; left scale) compared to LLE and SLE counterparts (right scale). The dashed line separates the REEs and other relevant elements.

expected for a ligand with a large *bite angle*, it is less efficient for extracting smaller lanthanides.

However after grafting on solid surface, the hybrid material KIT-6-N-FDGA shows only a small perturbation in the  $K_d$  along the lanthanide series with little selectivity when comparing with the extraction of the other metals tested. Nevertheless, it is interesting to note that the  $K_d$  value for  $\text{Sc}^{3+}$  is surprisingly high, around  $11\,000\text{ ml g}^{-1}$  (Fig. 4C), which is unexpected since  $\text{Sc}^{3+}$  has an ionic radius which is quite distinct from those of all of the lanthanide ions, being much smaller ( $74.5\text{ pm}$ ).<sup>6</sup> This selectivity for the smallest REE suggests that another factor influences the interaction of the REE ions with the FDGA ligand upon grafting, since the latter species has the largest *bite angle* of the systems tested.

In order to get more insight into such discrepancy in the extraction properties, a first series of XPS analyses of pristine KIT-6-N-FDGA along with those of materials saturated with  $\text{Sc}^{3+}$  and  $\text{Gd}^{3+}$  were carried out. It was observed that the N 1s shift for  $\text{Sc}^{3+}$  ( $400.98\text{ eV}$ ) compared to the pristine material ( $400.10\text{ eV}$ ) was much more pronounced than the one observed for  $\text{Gd}^{3+}$  ( $400.50\text{ eV}$ ), suggesting that the interaction with  $\text{Sc}^{3+}$  is taking place with the N–H rather than the C=O typically observed for lanthanide coordination with DGA-type ligands, which would explain the different selectivity.<sup>12</sup> However, this coordination mode is quite unusual and homogeneous models have yet to be synthesized to learn more about this bonding type.

Additionally, a comparison of the separation factors between selected elements, *i.e.*, Ce/La, Gd/La and Lu/La, for LLE and SPE techniques, using DOODA or FDGA, is given in Table S3, ESI.† It can clearly be seen that greater separation factors between these lanthanides and La were obtained for the SPE systems. For instance, Lu/La separation factor is only 0.3 for the LLE system, while in case of the mesoporous sorbents this factor is increased 6 times.

Finally, in order to study the stability of the hybrid organo-silica sorbents, several loading-release cycles, in the flow/dynamic system, were performed, as shown in Fig. 5. These multiple adsorption-desorption cycles confirmed the high

stability of the organo-silica resins under the extraction conditions tested.

## Conclusions

In summary, by a careful tuning of the *bite angle* of chelating ligands and by imparting rigidity to the ligands on a surface, a more selective extraction of lanthanides can be achieved. The DOODA ligand grafted on mesoporous silica (KIT-6) has a smaller *bite angle* than the DGA ligand and shows preference for extracting smaller lanthanides (Ho–Lu). Interestingly, after immobilizing FDGA, exceedingly high  $K_d$  values were obtained for extracting scandium from a mixture of REEs. The critical role of the support is discernible when comparing the extraction behaviour of these ligands in LLE and the grafted systems. Obviously, it is certainly possible to further tune the *bite angle* by changing the ligand structure, aiming at a selectivity for other elements. Importantly, experiments under non-equilibrium conditions such as flow-through system will also be needed for mimicking extraction conditions and study kinetic effects, which could affect performances. Finally, these new materials will have to be tested in real practical settings for the mining industry or to valorise wastes by “urban mining”.

## Acknowledgements

The authors wish to acknowledge the Fonds Québécois de Recherche Nature et Technologies Québec (FRQNT) and National Sciences and Engineering Research Council of Canada (NSERC) for financial support.

## Notes and references

- (a) J. C. G. Bünzli and C. Piguet, *Chem. Soc. Rev.*, 2005, **34**, 1048–1077; (b) L. D. Carlos, R. A. S. Ferreira, V. Z. Bermudez and S. J. L. Ribeiro, *Adv. Mater.*, 2009, **21**, 509–534; (c) K. Binnemans, *Chem. Rev.*, 2009, **109**, 4283–4374; (d) R. Sessoli, *Angew. Chem., Int. Ed.*, 2008, **47**, 5508–5510; (e) N. Ishikawa, M. Sugita, T. Ishikawa, S. Y. Koshihara and Y. Kaizu, *J. Am. Chem. Soc.*, 2003, **125**, 8694–8695; (f) A. R. Rocha, V. M. García-Suárez, S. W. Bailey, C. J. Lambert, J. Ferrer and S. Sanvito, *Nat. Mater.*, 2005, **4**, 335–339.
- (a) T. Zhu, *Hydrometallurgy*, 1991, **27**, 231–245; (b) M. L. P. Reddy, P. Rao and A. D. Damodarm, *Miner. Process. Extr. Metall. Rev.*, 1995, **12**, 91–113; (c) W. Li, X. Wang, H. Zhang, S. Meng and D. Li, *J. Chem. Technol. Biotechnol.*, 2007, **82**, 376–381; (d) J. D. S. Benedetto, M. L. Soares, I. Greval and D. Dresinger, *Sep. Sci. Technol.*, 1995, **30**, 3339–3349.
- (a) B. R. Reddy, S. Radhika and B. N. Kumar, *Chem. Eng. J.*, 2010, **160**, 138–144; (b) S. K. Menon, H. Kaur and S. R. Dave, *React. Funct. Polym.*, 2010, **70**, 692–698; (c) Q. Jia, Z. H. Wang, D. Q. Li and C. J. Niu, *J. Alloys Compd.*, 2004, **374**, 434–437; (d) B. Kronholm, C. Anderson and P. R. Taylor, *JOM*, 2013, **65**, 1321–1326.

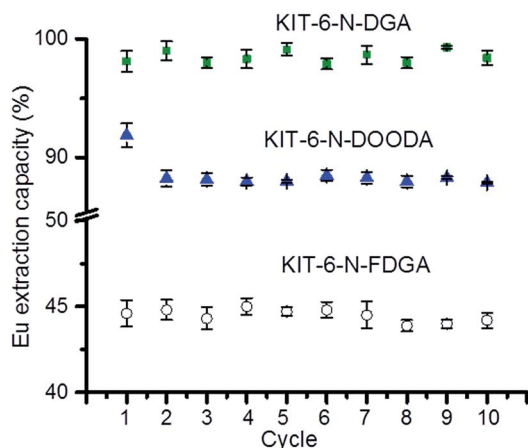


Fig. 5 Reusability of the functionalized mesoporous silica sorbents after 10 extraction–release cycles, in the dynamic system.

- 4 A. Zhang, C. Mei, Y. Wei and M. Kumagai, *Adsorpt. Sci. Technol.*, 2007, **25**, 257–272.
- 5 G. K. Schweitzer and L. L. Pesterfield, *The aqueous chemistry of the elements*, Oxford University Press, New York, 2009.
- 6 S. Cotton, *Lanthanide and Actinide Chemistry*, John Wiley & Sons, Chichester, 2006.
- 7 (a) A. Abbasi, P. Lindqvist-Reis, L. Eriksson, D. Sandstrom, S. Lidin, I. Persson and M. Sandstrom, *Chem.–Eur. J.*, 2005, **11**, 4065–4077; (b) C. Cossy, L. Helm and A. E. Merbach, *Inorg. Chem.*, 1989, **28**, 2699–2703; (c) W. Meier, P. Bopp, M. M. Probst, E. Spohr and J. I. Lin, *J. Phys. Chem.*, 1990, **94**, 4672–4682.
- 8 (a) F. A. Hart, *Comprehensive Coordination Chemistry*, Pergamon Press, Oxford, 1987, vol. 3; (b) D. G. Karraker, *J. Chem. Educ.*, 1970, **47**, 424–430.
- 9 (a) F. Xie, T. A. Zhang, D. Dreisinger and F. Doyle, *Miner. Eng.*, 2014, **56**, 10–28; (b) K. A. Rabie, *Hydrometallurgy*, 2007, **85**, 81–86; (c) Y. C. Wang, S. T. Yue, D. Q. Li and C. Z. Li, *Solvent Extr. Ion Exch.*, 2002, **20**, 701–706; (d) D. K. Singh, H. Sing and J. N. Mathur, *Hydrometallurgy*, 2006, **81**, 174–181.
- 10 (a) H. Narita, T. Yaita, K. Tamura and S. Tachimori, *Radiochim. Acta*, 1998, **81**, 223–226; (b) Y. Sasaki, Y. Sugo, S. Suzuki and S. Tachimori, *Solvent Extr. Ion Exch.*, 2001, **19**, 91–103; (c) Z. X. Zhu, Y. Sasaki, H. Suzuki, S. Suzuki and T. Kimura, *Anal. Chim. Acta*, 2004, **527**, 163–168; (d) Y. Sasaki, P. Rapold, M. Arisaka, M. Hirata and T. Kimura, *Solvent Extr. Ion Exch.*, 2007, **25**, 187–204.
- 11 (a) Y. Sasaki, Z. Zhu, Y. Sugo and T. Kimura, *J. Nucl. Sci. Technol.*, 2007, **44**, 405–409; (b) S. Kannan, M. A. Moody, C. L. Barnes and P. B. Duval, *Inorg. Chem.*, 2008, **47**, 4691–4695.
- 12 (a) Y. Zhang, Y. Wang, N. Tang, M. Tan and K. Yu, *J. Coord. Chem.*, 2002, **55**, 1293–1299; (b) K. Matloka, A. Gelis, M. Regalbuto, G. Vandegrift and M. J. Scott, *Dalton Trans.*, 2005, 3719–3721; (c) G. Tian, J. Xu and L. Rao, *Angew. Chem., Int. Ed.*, 2005, **44**, 6200–6203.
- 13 (a) J. Jover, N. Fey, J. N. Harvey, R. Osborne and M. Purdie, *Organometallics*, 2012, **31**, 5302–5306; (b) M. N. Birkholz, Z. Freixa and P. W. N. Leeuwan, *Chem. Soc. Rev.*, 2009, **38**, 1099–1118; (c) Z. Freixa and P. W. N. Leeuwan, *Dalton Trans.*, 2003, 1890–1901; (d) T. Papp, L. Kollar and T. Kegl, *J. Quantum Chem.*, 2014, 1–5.
- 14 (a) C. Premlatha and S. Soundararajan, *J. Inorg. Nucl. Chem.*, 1980, **42**, 1783–1786; (b) L. Y. Gur'eva, A. K. Bol'sheborodova and Y. L. Sebyakin, *Russ. J. Org. Chem.*, 2012, **48**, 1047–1054.
- 15 M. Gomes, A. Gandini, A. J. D. Silvestre and B. Reis, *J. Polym. Sci., Part A: Polym. Chem.*, 2011, **49**, 3759–3768.
- 16 (a) P. J. Lebed, J. D. Savoie, J. Florek, F. Bilodeau, D. Larivière and F. Kleitz, *Chem. Mater.*, 2012, **24**, 4166–4176; (b) J. Florek, F. Chalifour, F. Bilodeau, D. Larivière and F. Kleitz, *Adv. Funct. Mater.*, 2014, **24**, 2668–2676.
- 17 F. Kleitz, S. H. Choi and R. Ryoo, *Chem. Commun.*, 2003, 2136–2137.
- 18 (a) F. Kleitz, F. Bérubé, R. Guillet-Nicolas, C.-M. Yang and M. Thommes, *J. Phys. Chem. C*, 2010, **114**, 9344–9355; (b) A. V. Neimark and P. I. Ravikovitch, *Microporous Mesoporous Mater.*, 2001, **44**, 697–707.
- 19 (a) M. Iqbal, J. Husken, W. Verboom, M. Sypula and G. Modolo, *Supramol. Chem.*, 2010, **22**, 827–837; (b) S. Usuda, K. Yamanishi, H. Mimura, Y. Sasaki, A. Kirishima, N. Sato and Y. Niibori, *Chem. Lett.*, 2013, **42**, 1220–1222.
- 20 (a) M. Thommes, *Chem. Ing. Tech.*, 2010, **82**, 1059–1073; (b) A. V. Neimark, P. I. Ravikovitch and A. Vishnyakov, *J. Phys.: Condens. Matter*, 2003, **15**, 347–365.
- 21 (a) Y.-C. Pan, H.-Y. Wu, G.-L. Jheng, H.-H. G. Tsai and H.-M. Kao, *J. Phys. Chem. C*, 2009, **113**, 2690–2698; (b) T. Shigeno, M. Nagao, T. Kimura and K. Kuroda, *Langmuir*, 2002, **18**, 8102–8107.
- 22 E. P. Horwitz, D. R. McAlister, A. H. Bond and R. E. Barrans Jr, *Solvent Extr. Ion Exch.*, 2005, **23**, 319–344.
- 23 (a) H. Narita, T. Yaita and S. Tachimori, *Solvent Extr. Ion Exch.*, 2004, **22**, 135–145; (b) Y. Sasaki, Y. Kitatsuji, Y. Tsubata, Y. Sugo and Y. Morita, *Solvent Extr. Res. Dev., Jpn.*, 2011, **18**, 93–101; (c) Y. Sasaki, Y. Morita, Y. Kitatsuji and T. Kimura, *Solvent Extr. Ion Exch.*, 2010, **28**, 335–349.
- 24 (a) H. Narita, T. Yaita, K. Tamura and S. Tachimori, *J. Radioanal. Nucl. Chem.*, 1999, **239**, 381–384; (b) Y. Sasaki and S. Tachimori, *Solvent Extr. Ion Exch.*, 2002, **20**, 21–34.
- 25 (a) E. A. Mowafy and D. Mohamed, *Sep. Purif. Technol.*, 2014, **128**, 18–24; (b) T. Yaita, A. W. Herlinger, P. Thiyagarajan and M. P. Jensen, *Solvent Extr. Ion Exch.*, 2004, **22**, 553–571; (c) S. Nave, G. Modolo, C. Madic and F. Testard, *Solvent Extr. Ion Exch.*, 2004, **22**, 527–551.